

Classification for non infected and infected ganoderma boninense of oil palm trees using ALOS PALSAR-2 backscattering coefficient

I C Hashim ^{1,*}, A R M Shariff ², S K Bejo ², FM Muharam ³ and K Ahmad ⁴

¹Geospatial Information Research Centre (GISRC), Level 6 Tower Block, Faculty of Engineering, Universiti Putra Malaysia (UPM), 43400 Serdang, Selangor, Malaysia.

²Department of Biological and Agriculture, Level 3, Faculty of Engineering, Universiti Putra Malaysia (UPM), 43400 Serdang, Selangor, Malaysia.

³Department of Agriculture Technology, Faculty of Agriculture, Universiti Putra Malaysia, 43400 UPM Serdang, Selangor Darul Ehsan, Malaysia.

⁴Department of Plant Protection, Faculty of Agriculture, Universiti Putra Malaysia, 43400 UPM Serdang, Selangor Darul Ehsan, Malaysia.

izrahayu@gmail.com

Abstract. Malaysia's monthly export of oil palm product in 2015 was 25,370,294 tonnes valued at about RM60 million. Consequently, Malaysia is now one of the leading manufacturers and exporters of palm oil and its derivatives in the world. However, oil palm plantations in Malaysia are now facing the threat of a Basal Stem Rot (BSR) disease that is caused by fungus called the *Ganoderma boninense*. This disease reduces oil palm production as an infected mature oil palm dies after 2-3 years of being infected. A decision tree classification approach is proposed in this study for discriminating between non infected and infected of *G. boninense* in oil palm tree using backscatter values of ALOS PALSAR 2 in FELCRA Seberang Perak 10, Kampung Gajah, Perak. The methodology involves (1) collection of ALOS PALSAR 2 image which include dual polarization HH (Horizontal - transmit and Horizontal - receive) and HV (Horizontal - transmit and Vertical - receive); (2) infection status of the oil palm trees in the study area that comprise 92 trees; and (3) image pre-processing that includes radiometric calibration, speckle filtering and linear conversion to dB. The final stage is the backscatter classification of *G. boninense* health status using the Decision Tree classifier. The overall accuracy for HH and HV backscatter classification were 45.65% and 56.52% respectively. Further investigations may need to be carried out to improve existing accuracy.

1. Introduction

Oil Palm trees in countries in South East Asia and Malaysia are vulnerable to various fungus attacks with the most common being the *G. boninense*, which will result in the Basal Stem Rot (BSR) disease. This disease has been one of the major culprits in the oil palm yield reduction throughout most of the production areas in the country. A list of 7 out of 15 species of *Ganoderma* from all over the world is from peninsular Malaysia [1]. *G. boninense* is the most dangerous type of *Ganoderma* in peninsular Malaysia [2]. The *G. boninense* disease progresses by halting the growth of an oil palm tree with unopened spear leaves and dry rotting of the internal tissue at the stem base. However, the disease is usually only noticed when it is already at the stage where it is critical. Some of the symptoms include holes in the trunk, wilting of the leaves, and production of fruiting bodies. Severe cases include fallen trees which poses an adverse effect on the plantation. A number of techniques for early detection have been designed such as the *Ganoderma* Selective Medium (GSM) [3], polymerase chain reaction-DNA (PCR-DNA) technique [4], enzyme-linked immunosorbent assay-polyclonal antibody (ELISA-PAb) [5], GanoSken Tomography [6], Field Spectroscopy [7] and Mid-infrared spectroscopy [8]. Overall, it has been to be very difficult to



find an accurate detection method [9]. Though, it is reported that plants with less than 20 % infection can still be saved with proper treatment [10]. Hence, it is important to mitigate the disease by having it detected as early as possible. This is just important to address the issue of *G. boninense* issue in oil palm plantation.

In 1960, remote sensing was first introduced and since then, it has been extensively used in various areas, especially to store layers of data regarding land usage and its elements. Optical remote sensing remains the most utilized due to its advantage in resolution, both radiometric and spatial. However, because of haze that has a regular occurrence in Malaysia and other countries in the South East Asia region, its usage would result in distortion of the imagery [11]. In contrast, remote sensing satellites using RADAR technology employ microwaves are able to broadcast through most cloud and haze. Hence, the backscattering signals obtained using RADAR remote sensing satellites are less influenced by weather conditions. The Synthetic Aperture Radar system, which transmits and receives microwave signals, provides complementary information for optical remote sensing. The backscattering signals from SAR are sensitive to the architecture and dielectric properties of land surfaces, such as plant canopy, built-up and soils [12]. The advantages of SAR images over optical data are more obvious in agricultural applications, as crops change rapidly during their growing seasons. The resulting SAR backscatter signals are primarily a function of the canopy structure such as: the orientation, shape and size of the fruit, stalks and leaves; the water content of the crop canopy; and the soil conditions. However, the structure and water content varies from crop to crop and changes with different stages of crop development. Therefore, SAR images have the potential to not only distinguish different crop types but also to monitor crop growing conditions. A number of studies have proved the capabilities of SAR data in crop condition monitoring and biophysical parameter retrieval [13-16]. Studies show that the sensitivity of SAR backscattering to crop conditions depends on the SAR sensor parameters (polarization, incidence angles and wavelength). Generally, SAR that have short wavelengths like the X-band (~3cm) and C-band (~6cm) has a lower chance of penetrating the canopy. This causes it to mainly interact with the uppermost part of the canopy layers. In contrast, L-band (~20cm) and P-band (~100cm) which have wavelengths that are longer are able to penetrate the vegetation cover down to the soil [17]. The depth of the penetration achieved relies on the biophysical parameters of the objects that cause the scatter within the layer of the vegetation (e.g., geometry, size and water content, of the scatter objects) which might enhance or attenuate the interactions between microwaves and scatter-producing features.

The classification is a way or method that uses labels or class identifiers that are connected to the pixels to construct a remotely sensed image based on their characteristics. This is such as the backscatter response of different frequency or polarization and other attributes such as texture or temporal signature. There are a few types of classification approaches use for crop mapping such as: Standard maximum likelihood [18], Neural networks [19], Random forest [20-21], Support vector machines [22], and Decision tree classification [23-24]. Decision tree classifiers however not been used widely in remote sensing and it offer advantages such hierarchical classifier. It can handle non parametric data and it also has the advantage of simplicity, flexibility, and computational efficiency [25]. This type of method of classification has the ability to do the automatic feature selection and complexity reduction function. Also, the information that concerns the predictive or generalization ability of the classification is easily understood and interpreted. Decision tree classifier involves three steps which are: splitting nodes; determining which nodes; and assigning class labels to terminal nodes. Labels are designated upon votes that are of the majority or weighted when there is an assumption that certain classes are more likely than others.

This study serves as a study to classify between non infected and infected *G. boninense* of oil palm tree using backscatter values of ALOS PALSAR 2 in the FELCRA Seberang Perak 10, Kampung Gajah, Perak. We used dual polarization HH (Horizontal - transmit and Horizontal - receive) and HV (Horizontal - transmit and Vertical - receive). In this study, we assess the potential of backscattering from ALOS Palsar 2 image combining with oil palm healthiness census comprise 92 trees to discriminate between non infected and infected of *G. boninense* in oil palm. A decision tree classifier was used to classify the non infected and infected of *G. boninense* in oil palm plantation.

2. Materials and Methods

2.1. Study area

One of the biggest estate plants in that is established in Malaysia is FELCRA. FELCRA manages the FELCRA Seberang Perak plantation estate. FELCRA Seberang Perak 10, which is the study area is

located at approximately latitude 4° 06' 01" N & 4° 6'44.00" N and longitude 100°53'7.00" E & 100° 53' 42" E.

2.2. Dataset description

The ALOS PALSAR 2 - PALSAR is L-band radar with 1.2GHz center frequency. It is equipped with dual polarization HH (Horizontal - transmit and Horizontal - receive) and HV (Horizontal - transmit and Vertical - receive). It has an imagery level of 1.5 with high sensitive polarimetric mode. The radar was developed by the Japan Aerospace Exploration Agency (JAXA). Data acquisition is shown in Table 1.

Table 1. Acquired satellite remote sensing data [26]

Satellite sensor	Date of acquisition	Level of process	Pixel Spacing	Radar Frequency Band	Polarizations
ALOS PALSAR 2	20/3/2017	1.5	6.25 m	L band	HH & HV

2.3. Field Survey Data

Gathering of the field data was done on 20 March 2017. The collection of non infected and infected G. boninense of oil palm census based on visual classification was the foundation of the field trips. The healthiness level of BSR infection of trees is identified based on the visual symptoms by the expert from MPOB shown in Table 2 and Table 3.

Table 2. Category and description of infection status of the oil palm trees.

Category	Description
Non Infected	Healthy palm, no foliage symptom (0%), no fruiting body
Infected	Foliage symptom more than 25%, produce fruiting bodies

Table 3. Number of trees based on infection status.

Category	No of tree
Non Infected	55
Infected	37
Total	92

2.4. Imagery processing

There three main image processing that involved in this study and the workflow of the processing is shown in Figure 1.

2.4.1 ALOS PALSAR 2 image processing. The Sentinel Application Platform (SNAP) was used to carry out the image processing. It is an open source software for exploiting ESA SAR missions, including SENTINEL-1, ERS-1 & 2 and ENVISAT, as well as third party SAR data from ALOS PALSAR 2, TerraSAR-X, COSMO-SkyMed and RADARSAT-2. The ALOS PALSAR 2 data processing methods are as follows; filtering technique: there is a need to filter to the radar imageries from noise and small patches over the palm plantation parcels prior before the analysis of data. Thus, to do a speckle filtering of the radar imageries an Enhanced Lee filter with a 3×3 kernel was utilized. Next, radar backscatter coefficients (σ°) must be converted from linear to dB e.g. pixel intensity values to physical quantities. Then, converting the data type from .dim format to .tiff format for next processing in ArcGIS software.

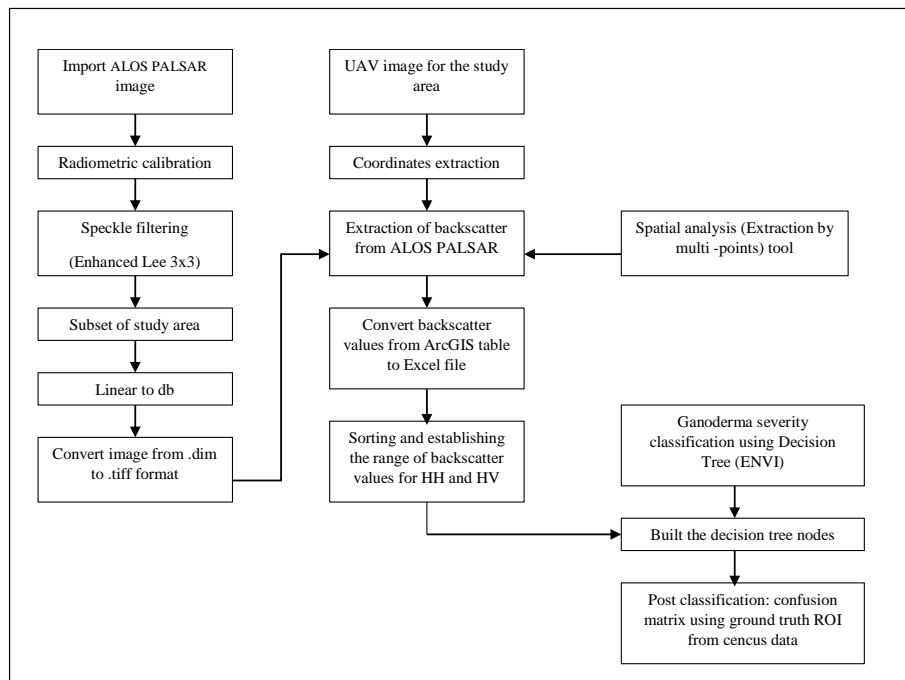


Figure 1. Image Processing Workflow

2.4.2 *Determining radar backscatter values based on census data.* Extraction of backscatter values from ALOS PALSAR 2 data of study area uses the ArcGIS Spatial Analyst – Extraction by multi point tool. It sorts and establishes the range for backscatter values of each polarization, HH and HV of infection status of the oil palm trees.

2.4.3 *Classification of non infected and infected Ganoderma in the study area.* Classification of Ganoderma severity level uses the Decision Tree classifier in ENVI software to build the decision tree nodes for the non infected and infected Ganoderma classes. Post classification: confusion matrix using ground truth ROI from census data. The purpose of the classification in this study is to view the distribution of non infected and infected Ganoderma in the study area.

3. Result and analysis

3.1. Average backscatter coefficient in the study area

Table 4 shows the backscatter coefficient values from ALOS PALSAR 2 for HH and HV polarization in the study area.

Table 4. Backscatter Coefficient Values from ALOS-2 against non infected and infected Ganoderma from Census Data.

Category	Backscatter Values (HH Polarization)	Range	Backscatter Values (HV Polarization)	Range
Non infected	≥ -10.000		≥ -17.336	
Infected	< -10.000		< -17.336	

3.2. Distribution of non infected and infected ganoderma in the study area

The classification results using Decision Tree classifier produced different accuracies. The overall accuracy for HH backscatter classification (Table 5) and HV backscatter classification (Table 6) were 45.65% and 56.52% respectively. From the classification results, it was found that HV backscatter classification was better to differentiate the non infected and infected of Ganoderma in oil palm plantation.

Table 5. Error matrix computed for the HH backscatter classification

Class	Ground Truth (pixel)		
	Non infected	Infected	Total Classified Pixel
Non infected	23	18	41
Infected	32	19	51
Total ground truth	55	37	92
Producer accuracy (%)	41.82	51.35	
User accuracy (%)	56.10	37.25	

Overall Accuracy = (42/92) 45.65%
Kappa Coefficient = -0.0643

Table 6. Error matrix computed for the HV backscatter classification

Class	Ground Truth (pixel)		
	Non infected	Infected	Total Classified Pixel
Non infected	32	17	49
Infected	23	20	43
Total ground truth	55	37	92
Producer accuracy (%)	58.18	54.05	
User accuracy (%)	65.31	46.51	

Overall Accuracy = (52/92) 56.52%
Kappa Coefficient = 0.1192

4. Conclusion

From the classification results, it was found that HV backscatter classification was better to differentiate the non infected and infected Ganoderma in oil palm plantation with overall accuracy for HV backscatter 56.52%. Soil properties and plant structure were different among the various fields. Hence, this implies that σ° was influenced by complex interactions among soil and plant scattering and not simply by means of a correlation to a single variable. This is inclusive of differences in permittivity and geometry of plant components (trunk, frond, etc.).

For agricultural monitoring, cloud cover can play havoc with monitoring initiatives where soil and crop conditions change on daily if not hourly temporal scales, requiring frequent observation to track crop evolution. As has been repeatedly touted by enumerable research papers and scientific presentations, SAR sensors have a key advantage over their optical counterparts because; they are active sensors that propagate energy at longer microwave wavelengths; SAR data acquisition is unaffected by the presence of cloud cover; and is independent of solar illumination. This has greatly expanded the world of possibilities for agricultural monitoring utilizing SAR data. However, Ganoderma study to map the individual trees are still lacking in the field of SAR. This study has only focused on backscatter and census oil palm; thus, is limited the scope of study to those areas. Further studies should investigate various variables and parameters such as, moisture content, biomass etc., and their correlation with the ground data.

Acknowledgement

The authors would like to express our gratitude to JAXA-SAFE, MPOB and FELCRA Berhad Perak for giving us permission to conduct our research work. We would also like to thank them for providing us information and data that is vital for our research.

References

- [1] Turner P. 1981. Oil palm diseases and disorders. Kuala Lumpur: Published for the Inc. Society of Planters [by] Oxford University Press.
- [2] Khairudin H. 1990. Basal Stem Rot of Oil Palm: Incidence, Etiology and Control. Master. Universiti Pertanian Malaysia, Selangor, Malaysia.

- [3] Ariffin D, Idris S. 1993. A selective medium for the isolation of Ganoderma from disease tissues. In: PORIM International Palm Oil Conference Progress Prospects Challenges Towards the 21st Century (Agriculture).
- [4] Idris A S, Yamaoka M, Hayakawa S, et al. 2003. PCR Technique for Detection of Ganoderma (MPOB Information Series No.188,4).
- [5] Idris A S, Rafidah R. 2008. Enzyme Linked Immunosorbent Assay-Polyclonal Antibody (ELISA-PAb) (MPOB Information Series, No.430, 4).
- [6] Idris A S, Mazliham M S, Loonis P, et al. 2010. GanoSken For Early Detection of Ganoderma Infection in Oil Palm (MPOB Information Series TT No. 442, 4)
- [7] Izzuddin M A, Idris A S, Wahid O, et al. 2013. Field Spectroscopy for Detection of Ganoderma Disease in Oil Palm (MPOB Information Series, No.532, 4)
- [8] Liaghat S, Mansor S, Ehsani R, et al. 2014. Mid-infrared spectroscopy for early detection of basal stem rot disease in oil palm [J]. *Computers and Electronics in Agriculture*, **101**:48-54.
- [9] Hushiarian R., Yusof N, Dutse S. 2013. Detection and control of Ganoderma boninense: strategies and perspectives [J]. *SpringerPlus*, **2**(1): 555.
- [10] Meor Yusoff M S, Muhd Asshar Khalid, Idris A S. 2009. Identification of Basal stem Rot Disease in Local Palm Oil by Microfocus XRF [J]. *Nuclear and Related Technologies*, **6**(1):282-287.
- [11] Van Gelder J. 2004. Greasy Palms: European Buyers of Indonesia Palm Oil. [online] Available at: http://www.foe.co.uk/resource/reports/greasy_palms_buyers.pdf [Accessed 15 Sept 2017].
- [12] McNairn H, Champagne C, Shang J, et al. 2009. Integration of optical and Synthetic Aperture Radar (SAR) imagery for delivering operational annual crop inventories. [J]. *ISPRS Journal of Photogrammetry and Remote Sensing*, **64**(5):434-449.
- [13] Moran M, Inoue Y, Barnes E. 1997. Opportunities and limitations for image-based remote sensing in precision crop management. [J] *Remote Sensing of Environment*, **61**(3):319-346.
- [14] Shao Y, Fan X, Liu H, Xiao J, et al. 2001. Rice Monitoring and Production Estimation using Multitemporal RADARSAT [J] *Remote sensing of Environment*, **76**(3):310-325
- [15] Blaes X, Vanhalle L, Defourny P. 2005. Efficiency of Crop Identification Based on Optical and SAR Image Time Series [J] *Remote Sensing of Environment*, **96**(4):352-365.
- [16] Chakraborty M, Manjunath K R, Panigrahy S, et al. 2005. Rice Crop Parameter Retrieval Using Multi-Temporal, Multi-Incidence Angle Radarsat SAR Data [J] *ISPRS Journal of Photogrammetry and Remote Sensing*, **59**(5):310-322.
- [17] Ulaby F T, El-Rayes M A. 1987. Microwave Dielectric Spectrum of Vegetation-Part II: Dual-Dispersion Model [J] *IEEE Transactions on Geoscience and Remote Sensing*, **5**:550-557
- [18] Skriver H., Mattia, F, Satalino, G, et al. 2011. Crop classification using short-revisit multitemporal SAR data. [J] *IEEE Journal of Selected Topics in Applied Earth Observations and Remote Sensing*, **4**(2): 423-431
- [19] Stankiewicz K A. 2006. The Efficiency of Crop Recognition on ENVISAT ASAR Images in Two Growing Seasons. [J] *IEEE Transactions on Geoscience and Remote Sensing*, **44**(4): 806-814.
- [20] Deschamps B, McNairn H, Shang, J, et al. 2012. Towards Operational Radar-Only Crop Type Classification: Comparison of a Traditional Decision Tree with a Random Forest Classifier. [J] *Canadian Journal of Remote Sensing*, **38**(1): 60-68.
- [21] Loosvelt L, Peters J, Skriver H, et al. 2012. Random Forests as a Tool for Estimating Uncertainty at Pixel-Level in SAR Image Classification. [J] *International Journal of Applied Earth Observation and Geoinformation*, **19**:173-184.
- [22] Tan X H, Bi W H, Hou X L, et al. 2011. Reliability Analysis using Radial Basis Function Networks and Support Vector Machines. [J] *Computers and Geotechnics*, **38**(2): 178-186.
- [23] McNairn H, Shang J, Champagne C, et al. 2009. Terrasar-X And RADARSAT-2 For Crop Classification and Acreage Estimation. [J] *Geoscience and Remote Sensing Symposium*, **2**:898
- [24] Skriver H, Dall J, Le Toan T, et al. 2005. Agriculture Classification using POLSAR data. *ESA Special Publication*, **58**: 32
- [25] Friedl M A, Brodley C E. 1997. Decision Tree Classification of Land Cover from Remotely Sensed Data. [J] *Remote sensing of environment*, **61**(3): 399-409
- [26] Auig2.Jaxa.Jp. 2017. AUIG2 (Login) ALOS2-FBDR1_5RUD-ORBIT ALOS2152453530-170320_Cal.dim. [online] Available at: <https://auig2.jaxa.jp/openam/UI/Login> [Accessed 12 April 2017].